



PSB NASA IN 71-711
028156

NASA-TM-112833

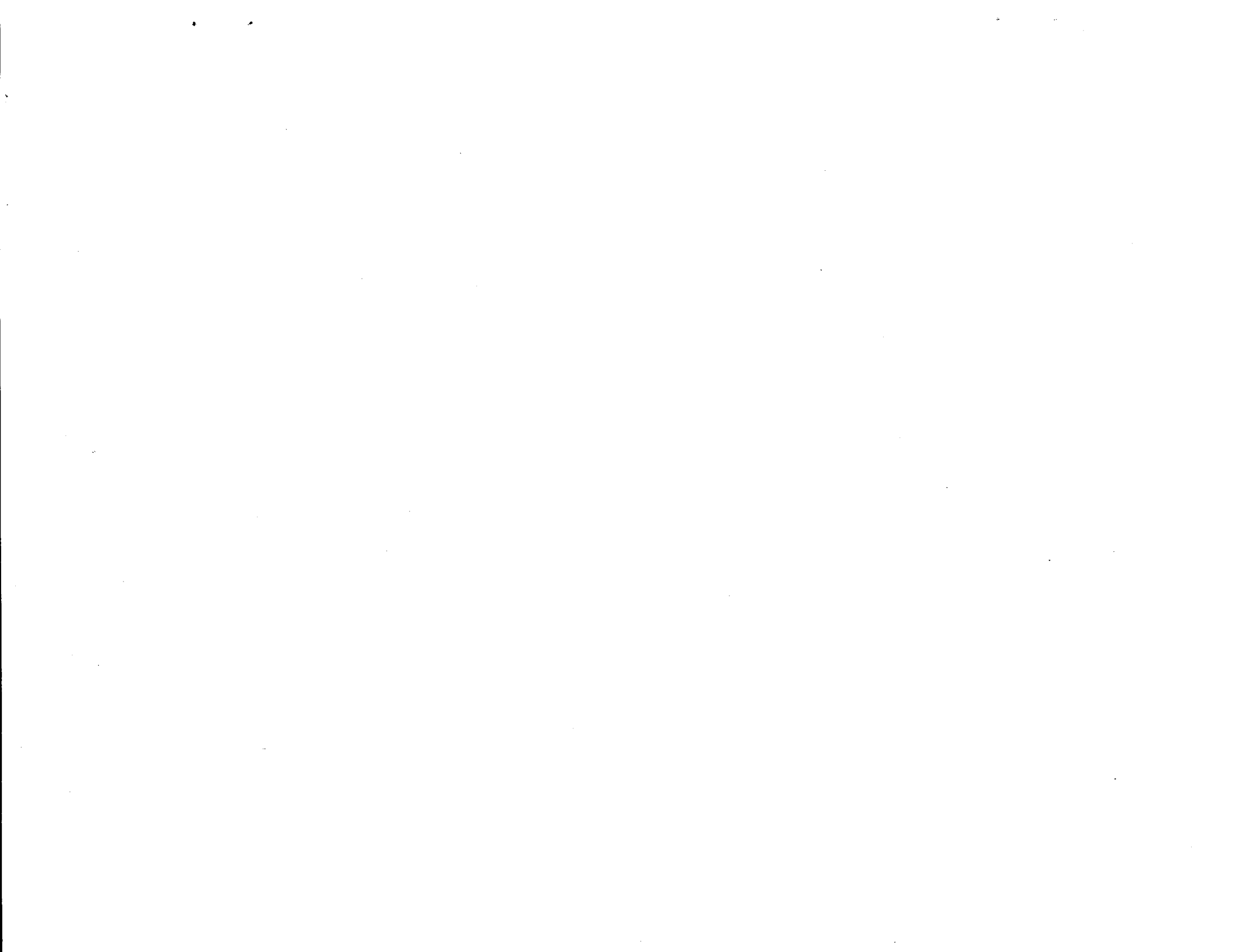
AIAA 97-1588

Azimuthal Patterns of the Radiated Sound Field from a Turbofan Model

**R. H. Thomas
Virginia Tech, VCES
Hampton, VA**

**F. Farassat, L. R. Clark, C. H. Gerhold
NASA Langley
Hampton, VA**

**3rd AIAA/CEAS Aeroacoustics Conference
May 12 - 14, 1997 / Atlanta, GA**



AZIMUTHAL PATTERNS OF THE RADIATED SOUND FIELD FROM A TURBOFAN MODEL

R. H. Thomas[†]

Mechanical Engineering Department, Virginia Tech
VCES, 303 Butler Farm Road, Suite 101, Hampton, VA 23666

F. Farassat^{††}, L. R. Clark^{*}, and C. H. Gerhold^{**}

MS 461, Aeroacoustics Branch, NASA Langley Research Center, Hampton, VA 23681

Abstract

The azimuthal directivity of a scale fan model was measured extensively. The model is a 12 inch diameter fan with 16 rotors and 40 stator vanes and tests were done at a tip speed of 905 ft/sec. Tests were conducted in an anechoic chamber with an inflow control device installed on the stationary fan model. The acoustic far field of the fan was surveyed with a circular hoop, with a diameter of six fan diameters, centered on the fan axis and was moved along the fan axis at polar angles from 20 to 110 degrees in increments of 10 degrees. The hoop, with 16 microphones evenly spaced at intervals of 22.5 degrees was rotated in 24 increments in the azimuthal direction for a total 384 points. From this extensive mapping of the directivity it is shown that the azimuthal directivity of the fundamental and first two harmonics is significant and can vary up to 15 dB. The broadband can also have an azimuthal directivity with as much as a 4 dB variation. A theory is proposed which relates the radiated modes with the generation of the far field patterns which produce the azimuthal directivity.

Nomenclature

BPF	blade passage frequency
2BPF	first harmonic
3BPF	second harmonic
D	fan rotor diameter, 1.0 ft
ICD	inflow control device
SPL	Sound Pressure Level

[†] Research Assistant Professor, Senior Member, AIAA

^{††} Sr. Research Scientist, Associate Fellow, AIAA

^{*} Aerospace Engineer

^{**} Sr. Research Engineer, Member, AIAA

x	axial coordinate
ϕ	polar angle relative to engine axis
θ	azimuthal angle around engine axis

Introduction

The vast majority of far field acoustic testing of turbofan engines has assumed axisymmetry of the radiated sound field about the axis of the engine. This is logical given the fact that the turbofan is a basically axisymmetric machine. In fact, almost exclusively, far field acoustic surveys of full scale turbofan engines or of scale models are made using one of two basic formats, both assuming axisymmetry. For full scale engines, measurements are made at a constant radius from a polar angle of 0 to 160 degrees, typical, in the horizontal plane through the engine axis. For scale models, especially for wind tunnel testing, measurements are made in a sideline traverse along a line at a constant distance from the engine axis. It appears that in most engine or model fan tests that symmetry about the axis is not even checked for.

However, azimuthal directivities have been observed in some cases. For the similar case of counter-rotating propellers a helical pattern was observed in the far field.¹ For this case a theory was developed for the acoustic interference pattern for propellers of equal blade number and rotational speed.² In an investigation of hybrid inlets on a JT15D engine measurements were made in two azimuthal angles and did show considerable variation but were not investigated further.³

The authors recently tested the same 12 inch fan model used in this investigation in a wind tunnel

Copyright © 1997 by the American Institute of Aeronautics and Astronautics, Inc. No copyright is asserted in the United States under Title 17, U.S. Code. The U.S. Government has a royalty-free license to exercise all rights under the copyright claimed herein for government purposes. All other rights are reserved by the copyright owner.

and measured large azimuthal variations in the far field of the fan as measured by 15 sideline microphones each at a different azimuthal angle.⁴ These variations at the BPF tone were attributed to standing wave patterns in the far field caused by the interaction of counter-rotating modes. These counter-rotating modes were attributed to rotor-stator interaction modes interfering with extraneous modes produced by an interaction between the rotor and a nonuniform rub strip. However, at the 2BPF tone where large variations were also present, it was not clear how the extraneous modes could propagate in order to create standing wave interaction with the single propagating mode due to rotor-stator interaction.

Recently, Ganz published very clear results of azimuthal directivity measurements also on a 12 inch fan model tested with an inflow control device.⁵ In this study, cylindrical rods were placed upstream of the rotor to create an inflow-rotor interaction. Measurements were taken in the far field in both polar and azimuthal angle but only for the BPF tone which was cut-off due to rotor-stator interaction but cut-on due to interaction with the rod wakes. Ganz showed that large azimuthal variation in the BPF tone level occurred when two spinning modes were propagating. The measurements also clearly showed that the annular period of the azimuthal variations was $2\pi(m_1 - m_2)$ degrees, where m_1 and m_2 are two spinning modes. Ganz concluded that the large azimuthal variations would not be present if tones were dominated by only one spinning order.

It seems that only in ideal designs would there be cases where really only one circumferential mode was present. Considering the reality of a practical engine installation it would appear that extraneous modes will tend to be present. This situation would seem to make the presence of azimuthal patterns a strong possibility. This should motivate a more complete understanding of these patterns including all sources of their generation and propagation as well as the implications for the radiated far field. This is the purpose that this paper will contribute to.

Fan Model

The fan model used in this work is a 12 inch diameter fan which was scaled from the Pratt and Whitney 17 Inch Advanced Ducted Propeller model. The fan model was originally constructed in 1993 and details of the design and description of its features have been previously reported.^{4,6} Only relevant features will be described here.

The fan has 16 wide chord rotor blades with a hut-to-tip ratio of 0.445. In scaling from the 17 inch to the 12 inch model the tip speed was held constant, therefore the 100% design speed at standard atmospheric

conditions is 17188 rpm yielding a tip speed of 905 ft/sec. The blade angle setting is at the takeoff condition and the fan pressure ratio is 1.27 at the 100% speed.

Although the fan is capable of interchangeable stator vane sets the experiment reported here was done with a 40 vane stator set with a rotor-to-stator spacing of 2.0 based on the rotor mid-span chord. This stator vane set is a cut-off design for the BPF tone.

The rub strip has been identified in the past as a potential interaction source due to nonuniformity in the tip clearance.⁴ The rub strip used in this experiment had a static tip clearance of 0.030 inch with a maximum circumferential variation of 0.002 inch. In addition, the rub strip was constructed in a way such that there were no joints or discontinuities in either the circumferential or axial direction in the part of the rub strip which is closest to the rub strip.

The fan cowl is a flight type cowl whose internal contour was scaled from the Pratt and Whitney 17 inch model. The stator assembly provides the only structural support for the cowl. An ICD is attached to the fan cowl on the exterior of the inlet. The purpose of the ICD is to control inflow turbulence in order to allow proper simulation of flight type noise characteristics in a static ground test facility which was used in this work. The ICD was modeled after the NASA Lewis design for a compact ICD.⁷ A schematic of the fan and ICD installation is shown in Figure 1.

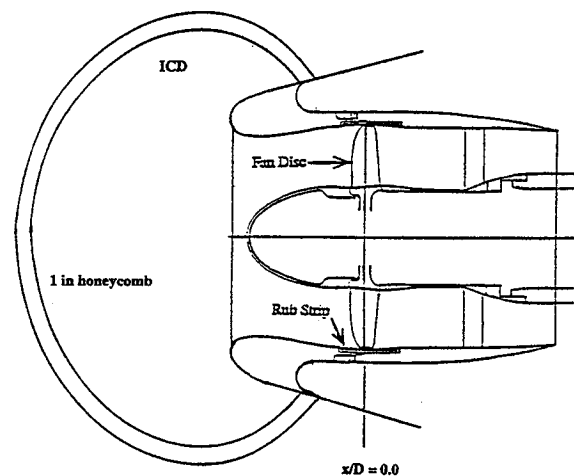


Figure 1. 12 inch fan with installation of the inflow control device.

Facility and Experimental Set-Up

The experiment was conducted in the Anechoic Chamber facility of NASA Langley Research Center. The internal dimensions of the test area (inside wedge tips) is 27.5 ft. by 27 ft. by 24 ft. The walls are

covered with wedges which are 3 feet thick and yields an adsorption coefficient above 99 percent above a frequency of 100 Hz. The 12 inch model is mounted on a truss structure in the corner of the facility in order to direct the turbine exhaust out of the anechoic chamber. Air is allowed in the chamber through an air inductor system in the roof of the chamber.

A microphone traverse system is part of the facility which allows for axial and azimuthal traverses. A circular hoop is mounted on a sled which can move in the axial direction on a ground track. The axial traverse can move the sled in the axial direction from $x/D = 2.0$ aft of the fan rotor to $x/D = 15$ in front of the fan. The $x/D = 0.0$ station is at the fan rotor stacking axis. Once at an axial location, the hoop can be rotated in the azimuthal direction. Installed on the hoop are 16 microphones evenly spaced for an angular separation of 22.5 degrees. This allows for complete coverage in the azimuthal direction in high resolution. Both the axial and azimuthal traverses are driven by stepper motors with precision of more than 1/100th of an inch. A schematic of the traverse system relative to the model is shown in Figure 2. Acoustic foam was installed around the axial traverse as much as possible and the hoop was covered in foam with a thickness of about 1 inch.

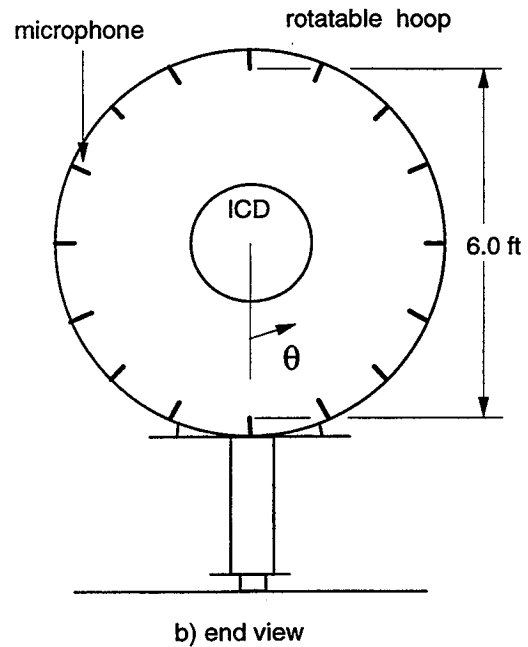
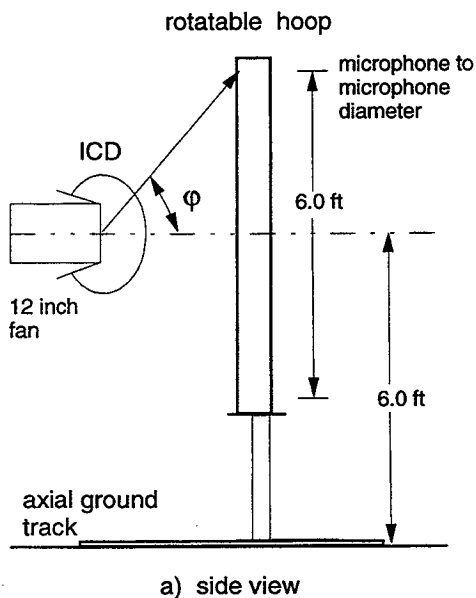


Figure 2. Rotable microphone hoop, a.) side view, b.) end view

Instrumentation and Data Analysis

The acoustic sensors used were 16 Brüel and Kjaer 1/2 inch microphones mounted on the circular hoop. The microphone signals were sampled at 62.5 kHz and low pass filtered at 30 kHz and high pass filtered at 300 Hz. At each measurement point the microphones were sampled for 2 seconds simultaneously and recorded. Microphone calibration corrections were applied to the signals. The sound pressure level spectra were computed from 20 averages of fast Fourier transforms each of 8192 points. The spectra were computed up to 15 kHz, which is enough to include the 3BPF tone. The peak level of the BPF, 2BPF, and 3BPF tones were identified from the spectra. A 16/rev shaft mounted sensor was recorded along with the microphone signals from which the blade passage frequency could be identified exactly. Also, the overall sound pressure level for the broadband level was computed after the effects of the tones were removed.

Description of Experiment

The experiment consisted of an extensive measurement of the radiated sound field of the 12 inch fan at one operating condition. The corrected speed of the fan was set at 17490 rpm and held within ± 70 rpm which corresponds to a 100% corrected speed condition. The hoop array of microphones was positioned at axial stations which correspond to polar angles (ϕ) of 20, 30, 40, 50, 60, 70, 90, 100, and 110 degrees relative to the

fan axis. At each polar angle, the hoop was then rotated in the azimuthal (θ) angle. The hoop was rotated in 1 degree increments up to 22 degrees and then 0.5 degrees for the last rotation since the 16 evenly spaced microphones were separated by 22.5 degrees. Therefore, 24 points in the azimuthal angle were taken by each of the 16 microphones for a total of 384 points at each polar angle. With 9 polar angles measured, the total number of points in the far field was 3456. This has resulted in a thorough survey of the far field for this particular condition.

Results

The acoustic data collected for this experiment were reduced to the three tones, BPF, 2BPF and 3BPF, and the overall sound pressure level (OASPL) for the broadband after the tones were removed. The BPF frequency for the 100% speed is 4660 Hz. The OASPL level was calculated over a frequency range of 2-15 kHz. Plots for the three tone levels and for the OASPL will be shown for two of the nine axial stations. This will demonstrate how the azimuthal patterns vary with polar angle.

The first axial station for which data is presented corresponds to the polar angle of 20 degrees where $x/D = 8.24$. Figure 3 is the plot of the BPF tone as a function of azimuthal angle. It shows two very large lobes at azimuthal angles of 0 and 120 degrees. These lobes are more than 10 dB from peak to trough. Figures 4 and 5 show the azimuthal variation of the 2BPF and the 3BPF tones, respectively. It is difficult to visually identify patterns, however, the variation in level is more than 10 dB for both tones. The broadband OASPL is shown in Figure 6. A segment of data around the 160 degree mark in the azimuthal angle was left out due to a data acquisition error. Otherwise, the variation of the broadband level with azimuthal angle is considerable, about 3 dB.

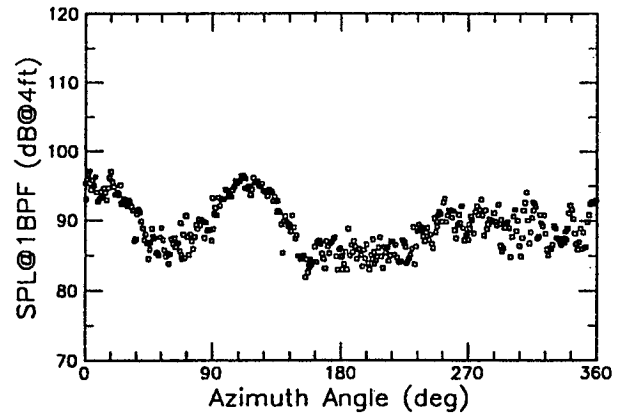


Figure 3. BPF tone level variation with azimuthal angle at $\theta = 20$ degrees.

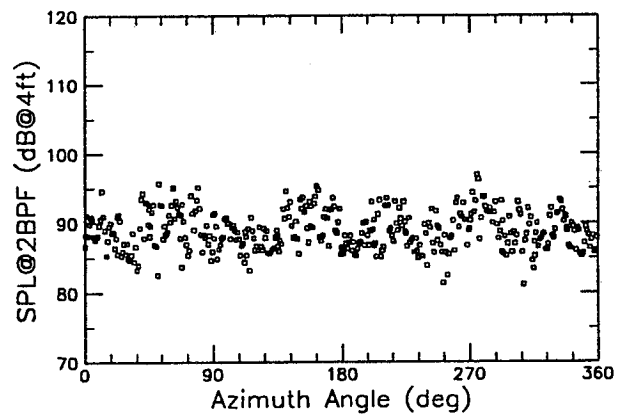


Figure 4. 2BPF tone level variation with azimuthal angle at $\theta = 20$ degrees.

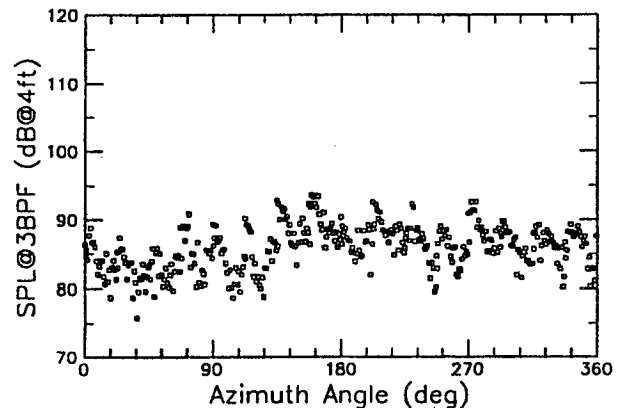


Figure 5. 3BPF tone level variation with azimuthal angle at $\theta = 20$ degrees.

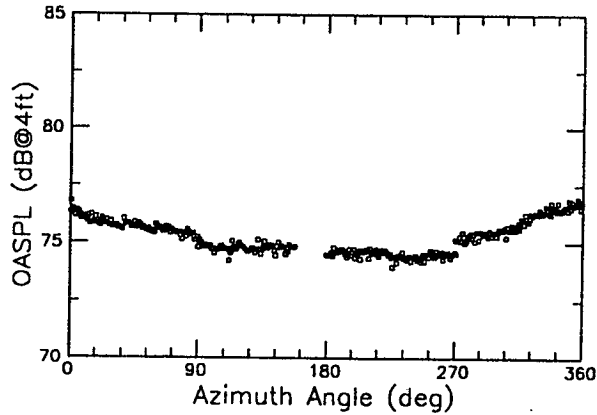


Figure 6. Broadband OASPL level variation with azimuthal angle at $\theta = 20$ degrees.

The measurement of the BPF tone sound pressure level at the single axial station of $x/D = 0.0$, which corresponds to a polar angle, $\phi = 90$ degrees, is presented in Figure 7 as a function of azimuthal angle. In the azimuthal direction it appears that there are 16 cycles in the BPF level, although some cycles are not so clear and the exact number may differ. The peak-to-trough of each cycle is as much as 12 dB.

The azimuthal measurement for the 2BPF is shown in Figure 8 and shows the same cyclical variation in the 2BPF tone level with azimuthal angle, however, the number of cycles is harder to visually identify. By this polar angle the 2BPF tone has fully cut-on and is some 15 dB above the level of the BPF tone.

In Figure 9, the azimuthal measurement of the 3BPF shows a greater peak-to-trough variation of 15 dB, however, visually it is not possible to identify specific cycles.

And finally, Figure 10 shows the measurement of the OASPL for the broadband. The azimuthal variation of the broadband is much less than for the tones, of course, however there is a variation of 2 dB at this angle, which still can be significant.

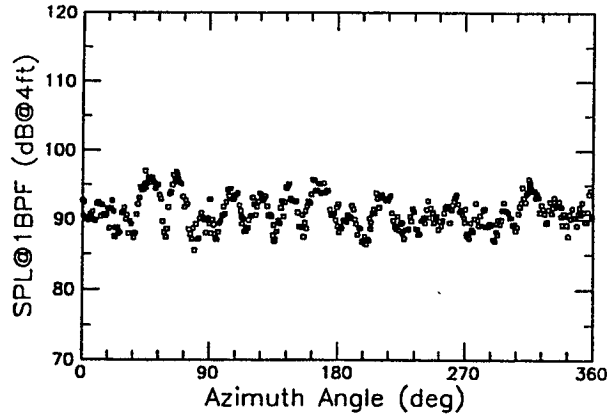


Figure 7. BPF tone level variation with azimuthal angle at $\theta = 90$ degrees.

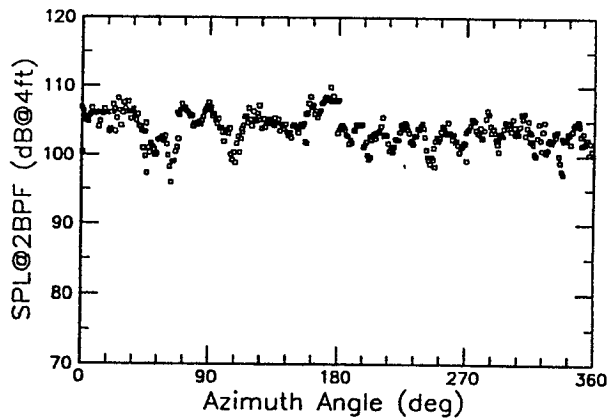


Figure 8. 2BPF tone level variation with azimuthal angle at $\theta = 90$ degrees.

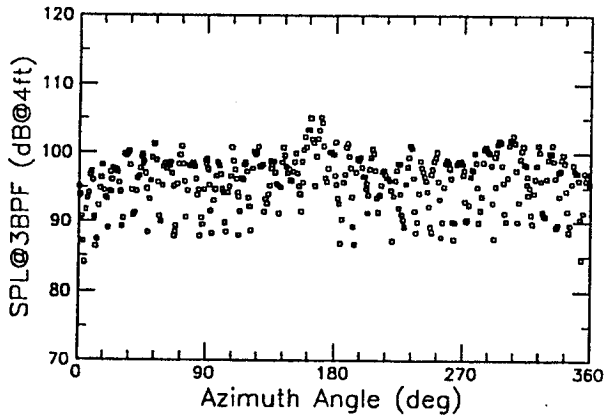


Figure 9. 3BPF tone level variation with azimuthal angle at $\theta = 90$ degrees.

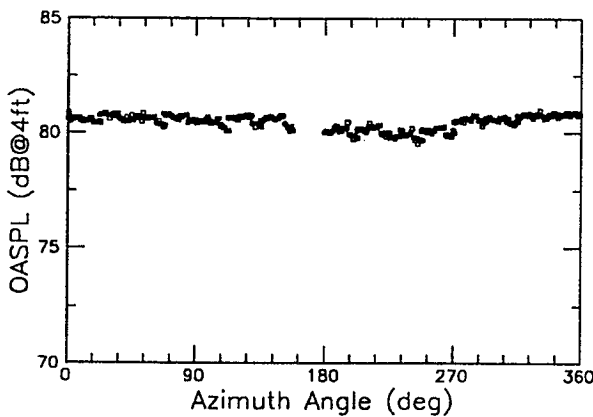


Figure 10. Broadband OASPL level variation with azimuthal angle at $\theta = 90$ degrees.

The above measurements were for just two polar angles. The 9 measured polar angle stations are combined and presented together in a contour plot in which the cylindrical measurement surface traced out by the rotating and translating hoop array is unwrapped into a flat contour plot surface. The BPF contour plot (not shown) has two areas in which there are significant cycles in the azimuthal direction. Close to the fan at polar angles of 70-90 degrees there appear to be the higher number of cycles, approximately 16 cycles. At lower polar angles, around 40 degrees, corresponding to $x/D = 4$, there appears to be a lower number of cycles in the azimuthal direction approximately 8 cycles. At 2BPF the tone is very strongly aft dominant, increasing

very sharply just aft of the fan at a polar angle of 90 degrees. Within the high levels of the 2BPF (also not shown) is very difficult to visually pick out cycles even though there is a variation in the tone by as much as 10 dB.

Figure 11, for the 3BPF tone, shows a pattern similar to that for the BPF tone in that there are two areas where the azimuthal variation is particularly noticeable, just aft of the fan from 90 to 110 degrees and in front of the fan at about 40 degrees. Near the fan the 40 cycle variation in the full 360 degrees of the azimuthal angle is particularly clear. In this contour format the 40 cycle pattern is very clear as compared to Figure 9 where the 40 cycle pattern was not visually evident. Close to the $x/D = 4$ station the number of cycles is less clear but it is between 30 and 40.

Finally for the broadband OASPL presented in Figure 12, the contour plot shows that the primary azimuthal variation occurs around the $x/D = 4$ station and is between 2-4 dB in magnitude. This azimuthal variation in the broadband level could be significant considering that small reductions in broadband levels produced by noise reduction concepts could be masked by this azimuthal variation.

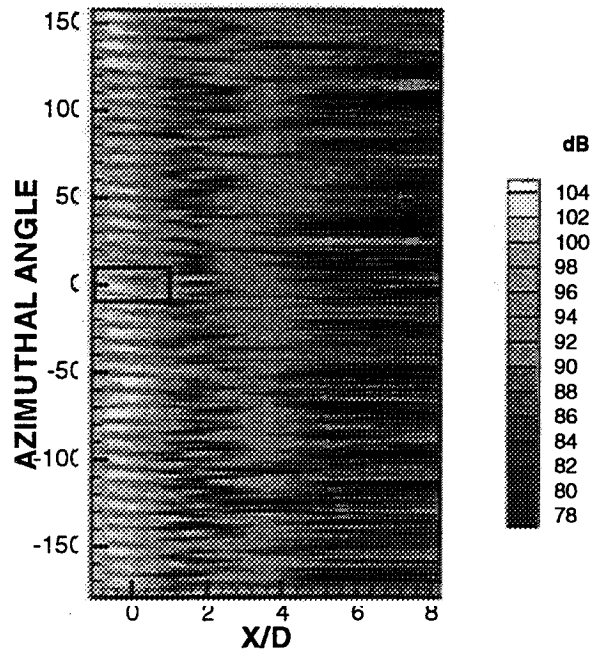


Figure 11. Contour of 3BPF tone level for all azimuthal and polar angles measured.

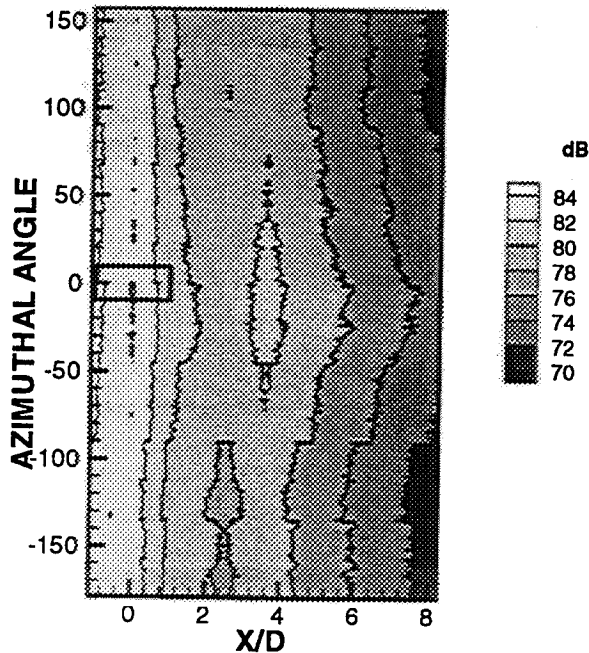


Figure 12. Contour of broadband OASPL levels for all azimuthal and polar angles measured.

Theoretical Analysis

The azimuthal patterns observed in the far field are fundamentally due to interference of some kind between multiple modes. These could be multiple modes from the same source such as the rotor-stator interaction or they could be from multiple sources including sources not yet identified or understood. Another possibility is that aft and forward radiated modes could interfere. This possibility of aft and forward mode interference will be eliminated in future experiments with a dividing wall eliminating the radiation path around the model exterior. The ability to detect and identify modes is essential to the understanding of azimuthal patterns. The next section presents the development of a method for the detection of modes.

Mode Detection by a Circular Microphone Array

A circular microphone array with center on the engine axis and in a plane perpendicular to the axis can be used to detect the modes that radiate from the inlet and the exhaust. We will first briefly discuss the theory of mode detection and then present the results of the

experiment described above for detecting the radiated circumferential modes. We follow the method presented by Farassat and Myers.⁸ Many researchers have proposed similar methods for mode detection.^{9,10}

We first introduce the following symbols:

r_o :	duct radius
α :	multiples of BPF
B :	number of blades
V :	number of stator vanes or number of circumferentially periodic disturbances
φ :	microphone angle from duct axis as seen from the center of the duct at inlet or exhaust
ρ_o :	density of the undisturbed medium
c :	speed of sound in the undisturbed medium
$m = \alpha B + qV$:	circumferential mode number, $\alpha = 1, 2, 3, \dots$, $q = \pm 1, \pm 2, \dots$
n :	radial mode number
Ω :	angular velocity of the rotor
θ :	azimuthal angle of the spinning mode
θ' :	azimuthal angle variable on the microphone array of an individual microphone
k_r :	radial wave number
R_o :	distance from duct center at inlet or exhaust to the microphone
a :	radius of microphone array,
x :	axial distance from inlet or exhaust

The acoustic pressure of the mode (m, n) at the inlet or exhaust $(x = 0)$ is given by

$$p'_s = e^{i\alpha B(\Omega t - \theta)} \sum_n \sum_q A_{nq} J_m[k_r(m, n)r] e^{-iqV\theta} \quad (1)$$

Note that q is the index of summation in this equation. It is a more convenient index for circumferential mode than m .

Using the Rayleigh's formula for radiation of the mode to the exterior region of the duct, the acoustic pressure at microphone position (a, θ', x) is given by

$$p'(a, \theta', x, t) = \frac{i}{4\rho_o R_o} D(\theta', x) e^{i\alpha B[\Omega(t - R_o/c) - \theta']} \quad (2)$$

where

$$D(\theta', \varphi) = \sum_q D_q(\varphi) e^{-iqV\theta'}, \quad (3)$$

$$D_q(\varphi) = \sum_n k_a(m, n) C_{mn}(\varphi) A_{nq} \quad (4)$$

and

$$C_{mn}(\varphi) = \int_0^{r_0} r J_m[k_r(m, n)r] J_m\left[\frac{\alpha B \Omega r}{c} \sin \varphi\right] dr \quad (5)$$

The complex Fourier transform in time t of the acoustic pressure at a fixed axial position x gives

$$\hat{p}(a, \theta', x, \alpha) = \frac{i}{8\pi\rho_0 R_0} e^{-i\alpha B \Omega R_0 / c} [e^{-i\alpha B \theta'} \sum_q D_q(\varphi) e^{-iqV\theta'}] \quad (6)$$

The term in front of the square brackets is a constant complex number. The function inside the source brackets is a periodic function of θ' with circumferential periodicity $2\pi/V$. This function can be Fourier analyzed to find all positive and negative q 's. This gives all radiating circumferential modes. The radiating radial modes can be identified by finding $D_q(\varphi)$ at several axial positions x and then solving a system of linear equations for A_{nq} using singular value decomposition.

We now report here the results this of analysis for the experiment described above for the circular microphone array using 16 microphones spaced at 22.5° along the circumference of the hoop. As this was a shakedown test of the array, no measurement of the phase difference between the microphones were performed. The test engine has 16 blades and 40 vanes ($B = 16$, $V = 40$). The inlet flow control device was used to break down the turbulence eddies entering the engine. This device was formed of 9 equal segments which produced 9 ribs on the spherical surface of the device. The sixteen microphones gave 384 circumferential measurements of the acoustic pressure which were Fourier analyzed in time at $\alpha = 1, 2, 3$ (i.e. BPF, 2BPF and 3BPF) to give the complex Fourier transform $\hat{p}(a, \theta', x, \alpha)$. This function was multiplied by $e^{i\alpha B \theta'}$ and Fourier analyzed in θ' to give the positive and negative q 's. From $m = 16\alpha + 40q$, the radiating circumferential modes were identified.

Figure 13 presents the result of an experiment at 100% speed with the microphone hoop array at the $x/D = 0$ axial location corresponding to a polar angle of 90° . At 3BPF ($\alpha = 3$), a clear 40 lobe pattern can be seen (see Figure 11) which is from $q = -1$; equivalent to circumferential mode number $m = 48 - 40 = 8$. This mode is certainly due to rotor-stator interaction. Other circumferential modes are also detectable but their cause

has not been identified. Figure 14 presents the result of circumferential mode identification at 3BPF ($\alpha = 3$) and $V = 9$. This analysis will identify the effect of the 9 ribs on the surface of the inlet flow control device on the noise. We get large amplitudes at $q = -8, -7, -6$ and -5 . These values of q correspond to circumferential modes of $m = -24, -15, -6$, and 3 . Clearly these modes are caused by the interaction of the wakes from the ribs with the rotor blades.

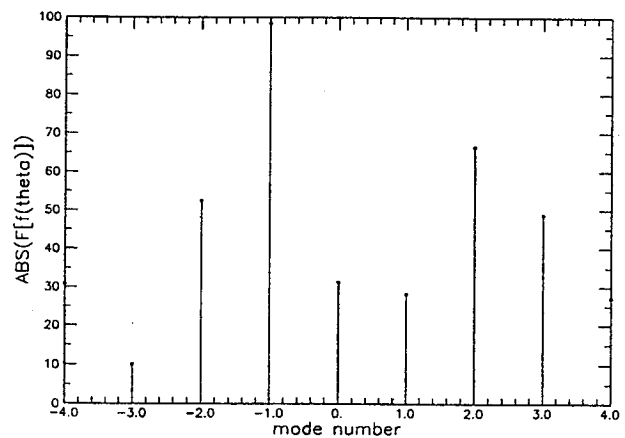


Figure 13. Fourier analysis in θ' of the 3BPF tone far field data at the polar angle $\varphi = 90^\circ$ for rotor stator interaction at $v = 40$.

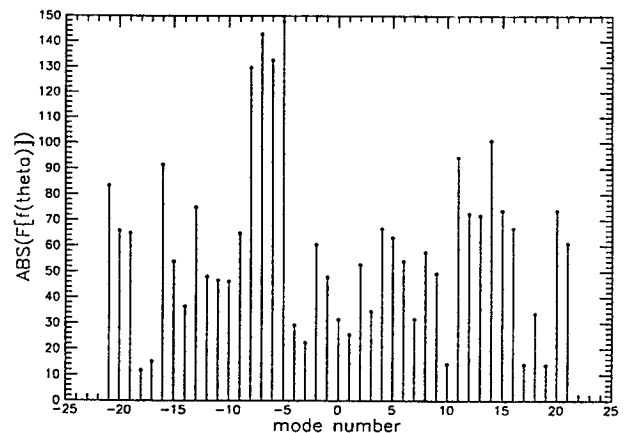


Figure 14. Fourier analysis in θ' of the 3BPF tone far field data at a polar angle of $\varphi = 90^\circ$ for the ICD rib rotor interaction with $v = 9$.

Conclusions

Using a translatable and rotatable hoop array of microphones, the far field of the NASA Langley 12 inch fan was extensively measured in the azimuthal angle with a resolution of one degree. Significant azimuthal variation has been measured of about 10-15 dB for the fundamental tone and first two harmonics and of 2-4 dB for the broadband levels. Obviously, the radiated sound field is nonaxisymmetric from a simple fan as used here even without struts, probes, or other obvious installation asymmetries. This should be a concern for the acoustic testing of fans.

The preliminary development of a method has been presented to detect modes in the far field. This method uses the data from the hoop array of microphones and Fourier analysis to determine the circumferential modes that have radiated into the far field. This method has been used to identify the $m = 8$ circumferential mode that originates from rotor-stator interaction and the $m = -24, -15, -6,$ and 3 circumferential modes that originate from the ICD rib-rotor interaction. Many more modes appear to be present. These could be generated by many additional sources. A likely source is the blade-to-blade variation in wake velocity deficit and spacing. This would effectively create a number of disturbances different from the actual number of stators. This could be a plausible source of the residual blade passage tone. These phenomena will be examined in the future with more extensive investigations now that the rotatable microphone array and mode detection method are operational.

Acknowledgements

The authors acknowledge the significant contribution during the course of this work of W. E. Nuckolls, D. W. DeVilbiss, and L. Becker. R. H. Thomas also gratefully acknowledges the support of this work by the Aeroacoustics Branch of NASA Langley.

References

- Block, P.J.W., "Installation noise measurements of model SR and CR propellers," NASA TM 85790, 1984.
- Tam, C.K.W., Salikuddin, M., and Hanson, D.B., "Acoustic Interference of Counter-Rotation Propellers," *Journal of Sound and Vibration*, Vol. 124, No. 2, 1988, pp. 357-366.
- Falarski, M.D. and Moore, M.T., "Acoustic Characteristics of Two Hybrid Inlets at Forward Speeds," *Journal of Aircraft*, Vol. 17, No. 2, 1980, pp. 106-111.
- Thomas, R.H., Gerhold, C.H., Farrasat, F., Santa Maria, O.L., Nuckolls, W.E., and DeVilbiss, D.W., "Far Field Noise of the 12 Inch Advanced Ducted Propeller Simulator," AIAA Paper No. 95-0722, 33rd Aerospace Sciences Meeting, Reno, NV, January 1995.
- Ganz, U., "Multi-Modal Directivities of Fan Tone Noise," NOISE-CON 96, Bellevue, WA, Oct. 1996.
- Hodges, R.M., Gerhold, C.H., Balster, D. and Thomas, R.H., "Acoustic Testing of Very High Bypass Ratio Turbofans Using Turbine Powered Scale Models," AIAA Paper 94-2552, presented at the 18th Aerospace Ground Testing Conference, June 20-23, 1994.
- Homyak, L., McArdle, J.G., and Heidelberg, L.J., "A Compact Inflow Control Device for Simulating Flight Fan Noise," AIAA Paper 83-0680, April 1983.
- Farrasat, F., Myers, M.K., "A Study of Wave Propagation in a Duct and Model Radiation," AIAA Paper 96-1677, presented at the 2nd AIAA/CEAS Aeroacoustics Conference, May 6-8, 1996, State College, PA.
- Heidelberg, L.J., and Hall, D.G., "Inlet Acoustic Mode Measurements Using a Continuously Rotating Rake," *Journal of Aircraft*, Vol. 32, No. 4, July-August, 1995.
- Joppa, P.D., "Acoustic Mode Measurements in the Inlet of a Turbofan Engine," *Journal of Aircraft*, Volume 24, No. 9, Sept. 1987.

